Oscillations in light-triggered logic microfluidic circuit

Citation: Cartas-Ayala, Marco A., Laura Gilson, Chong Shen, and Rohit Karnik. "Oscillations in light-triggered logic microfluidic circuit." Microsystem Technologies 20:3 (March 2014), pp. 437-444.

As Published: http://dx.doi.org/10.1007/s00542-013-1899-4

Publisher: Springer Berlin Heidelberg

Persistent URL: http://hdl.handle.net/1721.1/104803

Version: Author's final manuscript: final author's manuscript post peer review, without publisher's formatting or copy editing

Oscillations in light-triggered logic microfluidic circuit

Marco A. Cartas-Ayala, Laura Gilson, Chong Shen, Rohit Karnik*

Department of Mechanical Engineering, Massachusetts Institute of Technology, Cambridge MA, USA

*karnik@mit.edu

Phone: 617-324-1155

Abstract Control of droplets in microfluidic environments has numerous applications ranging from analysis and sample preparation for biomaterials synthesis (Mann and Ozin 1996) and medical diagnostics (Pipper et al. 2007) to photonics (Schmidt and Hawkins 2011). Here we study the oscillations present in a microfluidic circuit capable of sorting curable droplets on demand by triggering the circuit with UV-light. Prior to this paper we showed that a simple circuit can self-sort particles and produce a binary output, sorted or rejected stream of particles, based on the hydrodynamic resistance induced by the particles as they flow through the microfluidic channels. We showed that the cross-linking of droplets can modulate the resistance, and demonstrated particle switching by sorting of otherwise identical droplets of uncured and cured photocurable solution immersed in mineral oil solution. Before arriving at the sorting circuit, droplets made of a photocurable solution were illuminated by a UV-light from a mercury lamp, curing them. By tuning the outlet pressures, the switching threshold could be tuned so that uncured droplets were rejected while cured droplets were switched. (Raafat et al. 2010, Cartas Ayala et al. 2013). Here we use this system to study the oscillations in this circuit due to particle-particle interactions in the circuit. The circuit oscillation can be used as a counter with a light ON/OFF switch. The circuit behavior agrees well with theoretical predictions of droplet oscillations. Furthermore, the circuit oscillations can be switched on or off by UV-light illumination. This experiment demonstrates switching of particles based on deformability, illustrates the switching of particles by using light, and the possibility of creating new managing schemes for droplets by combining light control with droplet generation-rate control.

Keywords. *Lab-on-a-chip, droplets, UV-light, photocurable, deformability, mechanical properties*

1. Introduction

The control of microfluidic flows has gained increased attention in recent years, in particular the control of particles, e.g. droplets, in microfluidic channels. Droplets have numerous potential applications in the biological and physical sciences (Teh et al. 2008). Droplets can be used as vessels for minute biological samples, from single cells to small bacteria colonies (He et al. 2005), which provides the ability to heavily parallelize

experiments, decreasing experimental time and statistical uncertainty. Additionally, droplets can be used as micro-reactors in cases where chemicals are expensive or hard to obtain (He et al. 2005), and when a large set of conditions need to be explored, e.g. phase diagrams (Pompano et al. 2011; Salmon and Leng 2009). Further, understanding and controlling the formation of droplets in solution, i.e. emulsions, in highly controlled micro environments can potentially improve the production process of diverse products in which the microstructure is essential, ranging from shampoo to medicaments and enable the creation of novel products, such as nano and micro particles for therapeutics (Xu et al. 2009).

In order to perform experiments with a large number of droplets in microfluidic devices, the ability to control them dynamically is essential. For instance, when working with droplets that undergo reactions, divide (Jousse et al. 2006) or merge, the main goal is to obtain uniform and identical processing of the droplets except for the individual parameter that is probed, e.g. reaction time or cell viability. Nevertheless, processing of the droplets has unavoidable statistical variations that arise from different factors including imperfect droplet synchronization (Ahn et al. 2011), surface and interface effects, thermal and chemical gradients, etc., which generate undesired process variability. In such cases the ability to stop the process and remove the defective droplets is highly desirable.

Different methods have been proposed to enable droplet control at the micro scale. These methods can be classified as active and passive methods. Active methods require the incorporation of a sensor that probes droplet properties, e.g. fluorescence detectors, video cameras that monitor shape changes, or electrodes for measuring conductivity, and an actuation mechanism that forces droplets to change paths, e.g. PDMS-pneumatic valves (Lai et al. 2008) or electrodes (Link et al. 2006). Active methods have been demonstrated to be effective in different applications that require dynamic control, e.g. fluorescent cell sorting, but they are normally hard to integrate, consume large areas of the device or require large additional setups in addition to the microfluidic devices. In order to simplify integration, minimize cost and simplify on-chip processing, passive techniques have been developed (Gossett et al. 2010). In passive sorting techniques the droplets interact directly with the microfluidic environment to induce droplet paths modulated by the particle properties, e.g. inertial focusing (Beech et al. 2012; Di Carlo 2009).

The passive control of droplets at the microscale has evolved from simple T-junctions regulated by pressure (Thorsen et al. 2001; Vestad et al. 2004) to complex fully integrated devices that consider droplets and flows as logic units that can be analyzed and processed sequentially in parallel and in series and are regulated by droplet frequency and droplet arrival time. These techniques are globally known as microfluidic logic (Cheow et al. 2007; Prakash and Gershenfeld 2007). Current microfluidic logic relies on the interaction of multiple droplets to produce logic outputs, for example, by merging droplets or exploiting interactions between two or more droplets. Despite the large improvement over the initial control of microfluidic droplets, microfluidic circuits cannot be tuned easily on demand; the logic blocks are completely set once the device has been designed.

Here we use UV-light as a simple and effective method to turn ON and OFF microfluidic logic circuits, adding an additional dimension to existing microfluidic logic blocks (Cartas Ayala et al. 2013). We used a passive circuit, hence simple to integrate, that enables the sorting of photocurable microfluidic droplets based on the change in their mechanical properties that occurs upon curing. We used the induced hydrodynamic resistance, the resistance that a droplet generates as it is flowing through a microfluidic device, to act as a transducing property that transforms the droplet's mechanical characteristics into flow rate variations. Additionally, here we propose to use droplet-droplet interactions to create emergent droplet behaviors and provide additional functionalities to otherwise unaltered microfluidic circuits. This circuit can be potentially

used to sort droplet populations that contain cells, or reaction vessels whose properties change dynamically; further it can be used as a processing element that will complement the existing logic blocks available for microfluidic logic.

2. Materials and fabrication

2.1 Microfluidic devices

Devices were fabricated by standard micromolding in polydimethylsiloxane (PDMS, Sylgard 184, Dow Corning) using a SU-8 photoresist mold (Microchem). The molds were placed in a large covered Petri dish containing several drops of perfluorooctyltrichlorosilane (10 min) to facilitate removal of PDMS. PDMS was mixed (10:1 ratio) and poured into the mold (4 mm layer), degassed, and baked (80 °C for 30 min). The PDMS was removed, perforated to form the channel inlets using a biopsy punch (0.5 mm internal diameter punch from Harris Uni-Core), and cleaned using isopropanol. Finally, the PDMS component containing the channels was bonded to a clean glass slide using air plasma (30 s, 500 mTorr) (Expanded Plasma Cleaner, Harrick Plasma, Ithaca, NY). The devices were connected to constant pressure reservoirs via Tygon tubing. Two devices designs were used in the reported experiments.

2.2 Photocurable Droplets

Two solutions were used to produce droplets: an oil phase, carrier mix, and a water-soluble phase, droplet mix (Dendukuri et al. 2006). The oil phase was a mix of white light mineral oil (Mallinckrodt Chemicals) with Span 80 (1% v/v, Sigma Aldrich). The droplet mix comprised poly-ethylene glycol (400) diacrylate (67.5% v/v, Polysciences), hydroxy-2-methylpropiophenone (30% v/v, Sigma Aldrich), tween 20 (1.5% v/v, Sigma Aldrich), FITC BSA solution (1% v/vmL^{-1}, Sigma Aldrich), and a solution of fluorospeheres (1% v/v, Invitrogen carboxylated). A Nikon Eclipse TE2000-U inverted microscope with a Nikon Plan Fluor 10x/0.3 objective, a DAPI C100854 cube filter and an X-cite lamp, Series 120 were used to produce the UV spot.

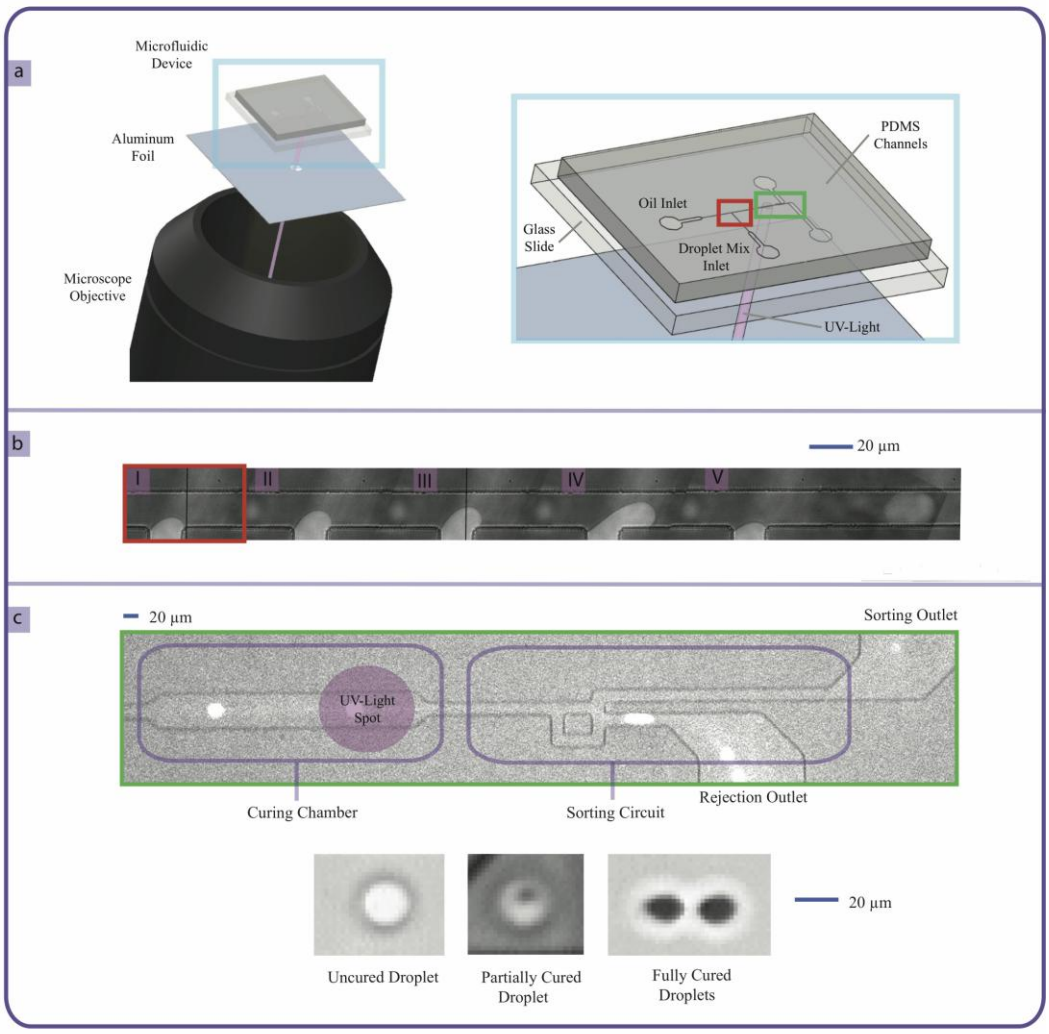

Fig. 1 Setup schematic. a) The microscope optical system is used to capture videos and produce the UV-light spot that cures the droplets. Aluminum foil with a ~1 mm aperture is used to minimize the undesired UV leakage that can potentially cure the inlet lines and other circuit areas. The inset shows a detailed view of the circuit. b) Droplets are formed at a T-junction upstream of the sorting circuit where the droplet mix and the oil carrier phase meet. c) After the droplets are produced at the T-junction, they enter an expansion chamber (curing chamber) that decreases their speed allowing for a higher exposure time for effective curing. Controlling UV-dosage is critical for proper device operation. Insufficient exposure will not cure the particles resulting in insufficient induced resistance to produce switching; overexposure will completely solidify the droplets causing clogging (see inset). Once the particles pass the curing chamber, they enter the sorting circuit where they are either selected or rejected.

3. Methods

3.1 Setup, droplet generation and droplet UV-curing

In order to cure droplets dynamically, the setup shown in **Figure 1** was used. The microscope optics used for imaging were also used to produce the ~100 μm UV-light spot to cure the microfluidic particles. In order to avoid UV-leakage that can potentially solidify the injection lines and other droplets in the device, an aluminum foil sheet with a ~1 mm aperture was positioned directly below the microfluidic device. The microfluidic device was manufactured as described in the materials section.

Droplets are produced in situ using a standard T-junction located upstream of the sorting circuit (**Fig. 1b**). In order to regulate the droplet frequency, the injection pressures of oil and droplet mix are controlled using a pressure regulator. After generation, droplets pass through a channel expansion, the curing chamber, in which the UV-light spot is located. The purpose of the curing chamber is to slow down the particles and increase the total UV-dosage received by the particles, facilitating proper droplet curing (**Fig. 1c**). If the particles are not cured, they do not exhibit sufficient hydrodynamic resistance to produce switching; if the particles are completely cured, they block the channels. In this manuscript we only sort partially cured droplets, and where we mention cured droplets, we imply partially cured droplets.

After passing through the curing chamber, the droplets, cured and uncured, are injected into the sorting circuit, where the particles are sorted according to their mechanical properties (**Fig. 1c**).

4. Results and discussion

The sorting circuit is formed by a Y-junction (sorting junction), formed by sensing, sorting and rejection channels, and a bypass channel which connects the sensing channel entrance to the middle of the rejection channel (**Fig. 2**). By design, the flow through the bypass channel is smaller than the flow through the sensing channel; hence when a droplet enters the sorting circuit it flows through the sensing channel. Also by design, the flow rate through the rejection channel is larger than the flow rate through the sorting channel. Hence, low-resistance particles (uncured droplets) flow through the rejection channel after passing through the sensing channel (Glawdel et al. 2011). When a cured droplet flows through the sensing channel, it induces a large hydrodynamic resistance, which alters the flows through the microfluidic circuit. As the cured particle flows through the sensing channel, the additional resistance reduces the flow through the sensing channel and increases the flow through the bypass channel. The increased flow through the bypass channel modulates the flow at the sorting Y-junction, generating a higher flow rate at the sorting channel and a lower flow rate at the first part of the rejection channel. The higher flow rate through the sorting channel, when compared to the flow through the rejection channel, drives the cured particles towards the sorting channel (Cartas Ayala et al. 2013).

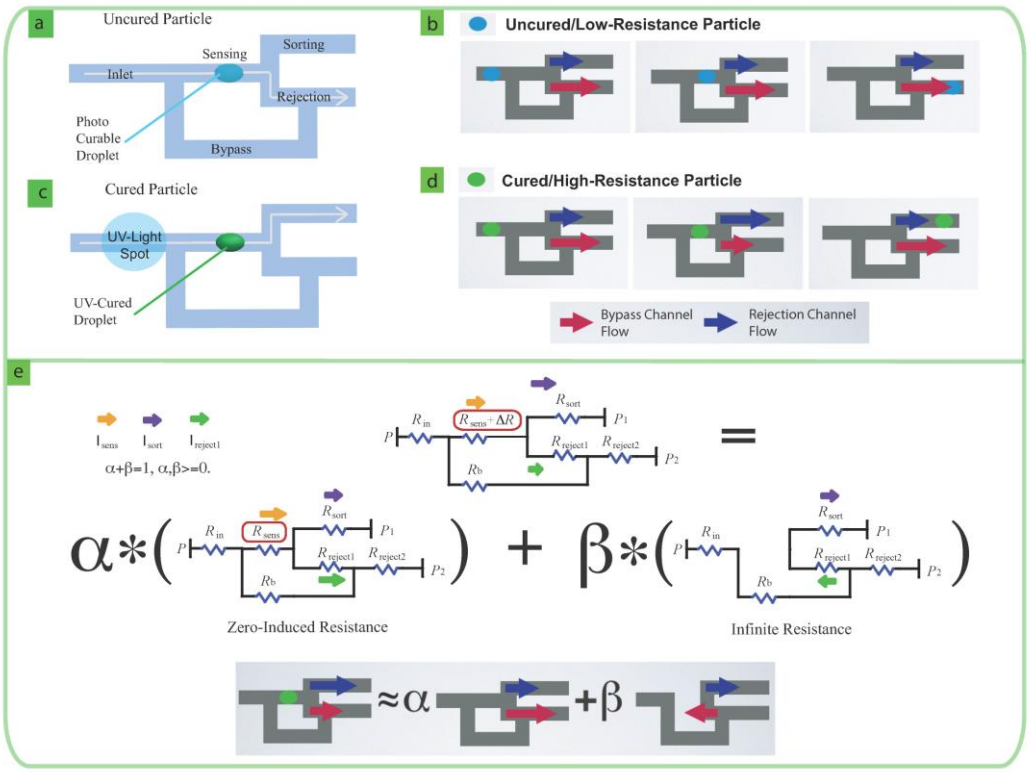

Fig. 2 Microfluidic circuit for self-sorting of droplets. The increased resistance in the Sensing Channel diverts the incoming flow into the Bypass Channel, thereby modulating the flows at the junction to result in particle sorting when the particle-induced resistance exceeds a threshold value. a) Trajectory of an uncured droplet with low hydrodynamic resistance. b) Schematic showing a low-resistance uncured droplet being rejected. Arrows indicate relative magnitudes of flows. c) Trajectory of a cured particle with high hydrodynamic resistance. d) Schematic showing a high resistance cured particle being sorted. e) Circuit schematic. The circuit operation during passage of a high-resistance cured droplet can be approximately understood as the superposition of the two flows: the undisturbed flows with no droplet flowing through and the flows of a droplet with infinite induced resistance. From these circuits it is clear that the flow through the first part of the rejection channel diminishes when a droplet increases the resistance in the sensing channel.

As a first approximation to understand the circuit behavior, we used the resistance model shown in **Fig. 2** (Cartas Ayala et al. 2013). Particle switching is achieved if the particle induces a hydrodynamic resistance, ΔR, greater than a threshold value such that the majority of the flow through the sensing channel flows through the sorting channel. Alternatively, switching is achieved if flow through the sorting channel is higher than the flow through the first part of the rejection channel. Hence, the circuit obeys the following logic:

$$\text{If } I_{sort} > I_{reject1}, \qquad (1)$$

the particle is sorted (*Output* = 1),

$$\text{If } I_{sort} < I_{reject1}, \qquad (2)$$

the particle is rejected (*Output* = 0).

In order to understand how the additional induced resistance modulates the flow rates and produces sorting, i.e. particle switching, we can visualize the flow through the circuit as a superposition of two circuits: a zero induced resistance circuit and an infinite induced resistance circuit (**Fig. 2e**). In the zero induced resistance circuit the flow through the first part of the rejection channel is larger than the flow through the sorting channel by design; hence the logic value is set to 0 by default. In the infinite resistance channel circuit, the sensing channel is effectively removed, which flips the flow direction through the first part of the rejection channel. A large, but finite, induced hydrodynamic resistance produces intermediate flow rates. Hence, the flow through the first part of the rejection channel decreases, while the flow through the sorting channel increases.

If the device is used for sorting particles, a single particle has to be analyzed at a time. The droplet generation frequency can be set to ensure single droplet analysis. If the time it takes to produce a droplet is larger than the time it takes for a droplet to flow through the sorting channel, i.e.

$$f^{-1} > \tau, \qquad (3)$$

where f is the generation frequency and τ is the sorting channel transit time, then a single particle is analyzed at a time. If the ratio $\tau * f > 1$, then droplets are generated faster than the rate at which they are analyzed, i.e. the rate at which they exit the sensing channel, and interactions between the particles arise.

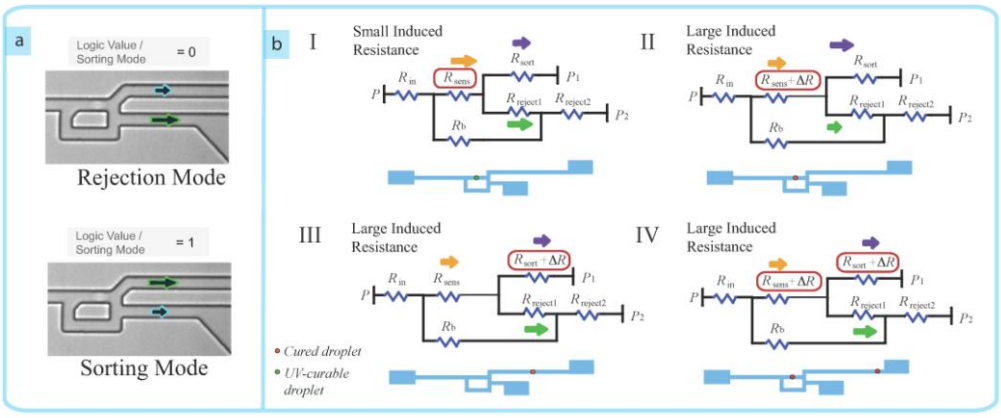

Fig. 3 Circuit states and droplet interference. a) The circuit has two logic values / operation modes depending of the relative magnitude of the flows in the sorting and first part of the rejection channels: Rejection Mode (0) and Sorting Mode (1). b) Droplet interaction can change the circuit's response depending on the droplet generation frequency. When two cured droplets that induce a hydrodynamic resistance larger than the threshold interact, the interaction can produce an oscillatory response of the circuit, passing from states I-IV depending on the droplets position.

Table 1: Applied Pressures.

Experiment	Droplet Mix Inlet Pressure (PSI)	Oil Inlet Pressure (PSI)	Sorting Channel Pressure (PSI)
1st Row	5.99	3.78	0.19
2nd Row	5.99	3.78	0.19

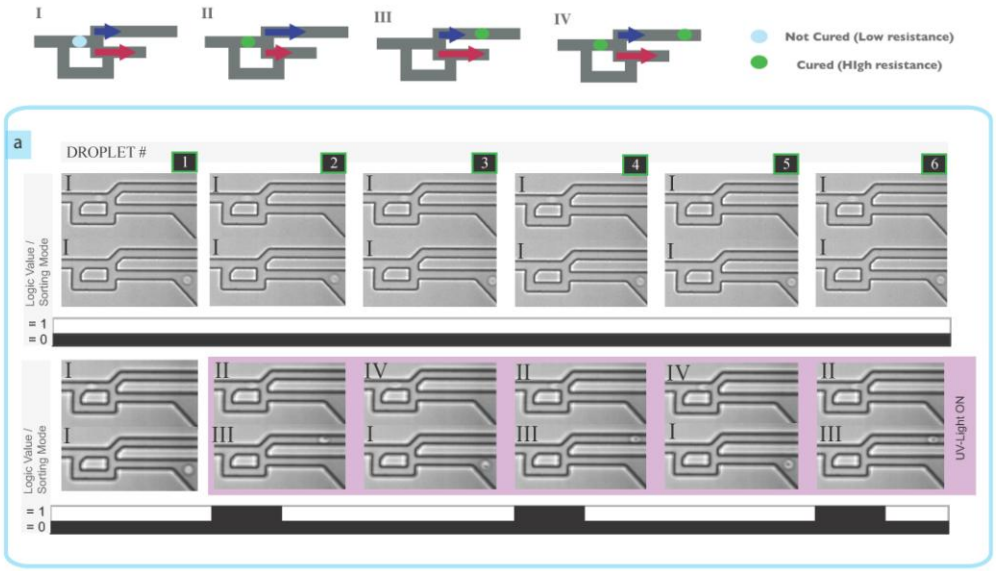

Fig. 4 Experimental verification of circuit states and droplet interference. a) Micrographs showing two sets of six continuous droplets. Note that each micrograph shows a single droplet, first as it travels through the sensing channel, and then as it exits the device after sorting. The first series of droplets (first row of micrographs) demonstrates the stability of the circuit when the UV-light is OFF. The second series oscillates from state I to IV after the UV-light is turned on; at the same time the sorting mode oscillates back and forth between logic level 0 and 1. Inset above figure shows droplet positions during their interactions (Notice state I can have either no particle flowing through the circuit or an uncured particle).

Particle interactions can be used to produce a digital oscillating signal with a frequency multiple of the droplet generation frequency that can be turned OFF and ON with light (**Fig. 3**). The circuit oscillates between two modes: rejection mode and sorting mode, which correspond to logic values (output values) of 0 and 1 respectively (**Fig. 3a**). When more than one particle passes through the circuit at a time, the circuit exhibits a more complex response than what we have described so far in terms of particle positions. For the case when only two particles interact at a time, and in order to understand the circuit behavior, we defined four additional states based on the possible particle interactions and positions; each one with a corresponding logic output value (**Fig. 3b**).

If the particle induces a small hydrodynamic resistance, i.e. the particle is uncured or the cured particle has exited the circuit, the circuit is in **state I** and the logic output value is 0. When a cured droplet traverses the sensing channel and no other particle is traversing the sorting channel, the circuit is in **state II**, which corresponds to a logic output value of 1. As the particle exits the sensing channel, it flows into the sorting channel since the logic value is 1. When a cured droplet traverses the sorting channel and no other particle is present in the sensing channel, the circuit is in **state III**. When a cured droplet flows through the sorting channel, it induces an additional hydrodynamic resistance in the sorting channel that increases the sorting threshold, i.e. increases the resistance required for the particles to switch the flow rates at the junction and alter the circuit's logic values. When a cured droplet traverses the sensing channel before the previous particle has exited

the sorting channel, the circuit is in **state IV**. As the particle exits the sensing channel, since the threshold resistance has increased, the particle is rejected.

Experimental verification of states I-IV is shown in **Fig. 4**, where $\tau * f = 1.3$ is shown. Pressures used during this experiment are shown if Table 1. The first row of **Fig. 2c** shows six consecutive uncured droplets flowing through the sorting circuit. The six droplets are rejected consistently, which demonstrates the stability of the circuit at the given pressure conditions; the circuit remains in state I. When the UV-light is turned ON a more complex behavior occurs. The circuit exhibits oscillations between different states, and switches consecutively from states I to IV and between logic values 0 to 1. The flow asymmetry between states II and IV, which correspond to logic values 0 and 1 respectively, creates oscillations in the in the sorting behavior. These oscillations occur due to the altered resistance once the UV-light is turned ON.

As the droplet generation frequency increases with respect to the sorting transit time, the cycle length, the time measure in droplets generated to produce a single oscillation in logic values, increases. Since the sorting channel is longer than the rejection channel, it takes longer for a sorted droplet to exit the device than a rejected droplet. When a particle travels through the sorting channel it modifies the flow rates forcing the device into the rejection mode. The rejection mode persists even if a particle travels through the sensing channel, since the circuit is more sensitive to changes in the rejection resistance than changes in the sensing resistance. Hence droplets can be sorted again only once the most recent sorted droplet has left the circuit. The cycle length in number of droplets is given approximately by

$$roof(\tau * f) = n_d \ , \quad (4)$$

where n_d is the number of droplets per cycle, and $roof(x)$ is a function that returns the next integer larger than x, a real positive number **(Fig. 5).**

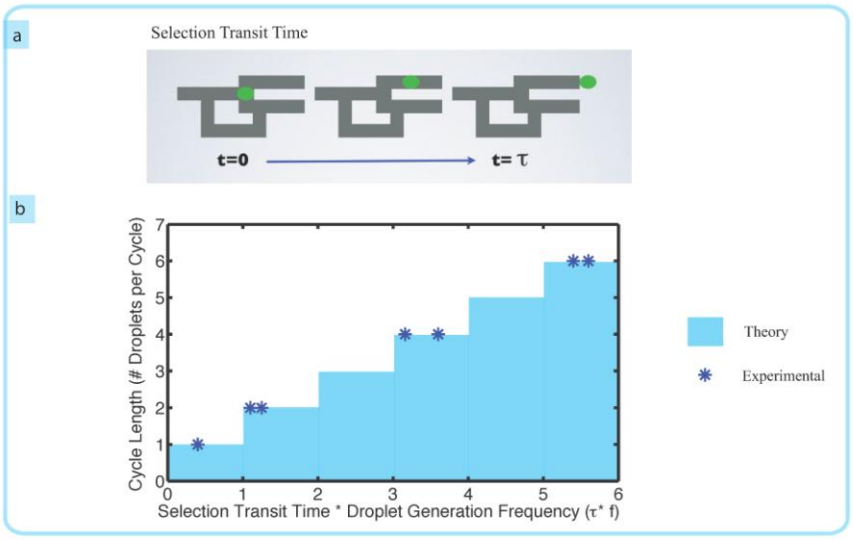

Fig. 5 Multiple Droplet Interactions. a) Droplet transition time. b) Cycle interaction length. Depending on the generation frequency and droplet velocity, droplets can interact before exiting the sorting circuit; the droplet-droplet interaction is cyclic: it repeats after a certain number of droplets pass by.

5. Conclusions

Here we illustrated particle sorting based on mechanical properties other than particle size and geometry, i.e. deformability, and that light can be used to trigger the switching between different circuit behaviors and logic outputs, i.e. the flow rates and droplet flow patterns can me modified by other means than imposing mechanically inlet pressure and/or flow rates. We have demonstrated that the circuit by itself is stable and curing the droplets entering the channel induces the switching behavior. We have developed a resistive model that permits understanding the changes in flow rates that the circuit experiences as cured droplets flow through. Finally, we have demonstrated that for a circuit whose cured-droplet transit time through the rejection channel is much smaller than its cured-droplet transit time through the sorting channel, the oscillation length of the logic value, measured in number of droplets, is determined by the ratio $\tau * f$. The circuit can find applications in microfluidic logic and other applications in which the use of extra mechanical parts to impose pressure and flow rates is constrained by space limitations, costs or other considerations. Further, the use of light to trigger circuits can add an additional dimension to "classical logic microfluidic circuits", making it possible to turn ON and OFF portions of the otherwise mechanically static processing units.

Acknowledgements We acknowledge financial support from the Mexican National Science Foundation, CONACYT grant 205899 (to M.C.A.) and the Lord Foundation (to L.G.). Devices were fabricated in the Microsystems Technology Laboratory (MTL) at MIT. We thank Evelyn Wang, for the use of the high-speed camera, and Todd Thorsen for helpful discussions.

References

Ahn B, Lee K, Lee H, et al. (2011) Parallel synchronization of two trains of droplets using a railroad-like channel network. Lab Chip 11:3956–3962. doi: 10.1039/C1LC20690G

Beech JP, Holm SH, Adolfsson K, Tegenfeldt JO (2012) Sorting cells by size, shape and deformability. Lab on a Chip 12:1048. doi: 10.1039/c2lc21083e

Cartas Ayala M, Gilson, L, Shen, C, Karnik R (2013) Self-sorting of deformable particles in an asynchronous logic microfluidic circuit. Small 9:375-381. doi: 10.1002/smll.201201422

Di Carlo D (2009) Inertial microfluidics. Lab Chip 9:3038–3046. doi: 10.1039/B912547G

Cheow LF, Yobas L, Kwong D-L (2007) Digital microfluidics: Droplet based logic gates. Applied Physics Letters 90:054107–054107–3. doi: doi:10.1063/1.2435607

Dendukuri D, Pregibon DC, Collins J, et al. (2006) Continuous-flow lithography for high-throughput microparticle synthesis. Nature Materials 5:365–369. doi: 10.1038/nmat1617

Glawdel T, Elbuken C, Ren C (2011) Passive droplet trafficking at microfluidic junctions under geometric and flow asymmetries. Lab Chip 11:3774–3784. doi: 10.1039/c1lc20628a

Gossett D, Weaver W, Mach A, et al. (2010) Label-free cell separation and sorting in microfluidic systems. Analytical and Bioanalytical Chemistry 397:3249–3267. doi: 10.1007/s00216-010-3721-9

He M, Edgar JS, Jeffries GDM, et al. (2005) Selective Encapsulation of Single Cells and Subcellular Organelles into Picoliter- and Femtoliter-Volume Droplets. Anal Chem 77:1539–1544. doi: 10.1021/ac0480850

Jousse F, Farr R, Link DR, et al. (2006) Bifurcation of droplet flows within capillaries. Phys Rev E 74:036311. doi: 10.1103/PhysRevE.74.036311

Lai C-W, Lin Y-H, Lee G-B (2008) A microfluidic chip for formation and collection of emulsion droplets utilizing active pneumatic micro-choppers and micro-switches. Biomedical Microdevices 10:749–756. doi: 10.1007/s10544-008-9186-3

Link DR, Grasland-Mongrain E, Duri A, et al. (2006) Electric Control of Droplets in Microfluidic Devices. Angewandte Chemie 118:2618–2622. doi: 10.1002/ange.200503540

Mann S, Ozin GA (1996) Synthesis of inorganic materials with complex form. 382:313–318. doi: 10.1038/382313a0

Pipper J, Inoue M, Ng LF-P, et al. (2007) Catching bird flu in a droplet. Nature Medicine 13:1259–63. doi: http://dx.doi.org.libproxy.mit.edu/10.1038/nm1634

Pompano RR, Liu W, Du W, Ismagilov RF (2011) Microfluidics Using Spatially Defined Arrays of Droplets in One, Two, and Three Dimensions. Annual Review of Analytical Chemistry 4:59–81. doi: 10.1146/annurev.anchem.012809.102303

Prakash M, Gershenfeld N (2007) Microfluidic Bubble Logic. Science 315:832–835. doi: 10.1126/science.1136907

Raafat MS, Cartas Ayala M, Karnik R (2010) Self-Sorting of Deformable Particles in a Microfluidic Circuit. μTAS Proceedings 1826–1828.

Salmon J-B, Leng J (2009) Microfluidics for kinetic inspection of phase diagrams. Comptes Rendus Chimie 12:258–269. doi: 10.1016/j.crci.2008.06.016

Schmidt H, Hawkins AR (2011) The photonic integration of non-solid media using optofluidics. Nature Photonics 5:598–604. doi: 10.1038/nphoton.2011.163

Teh S-Y, Lin R, Hung L-H, Lee AP (2008) Droplet microfluidics. Lab Chip 8:198–220. doi: 10.1039/B715524G

Thorsen T, Roberts RW, Arnold FH, Quake SR (2001) Dynamic Pattern Formation in a Vesicle-Generating Microfluidic Device. Phys Rev Lett 86:4163–4166. doi: 10.1103/PhysRevLett.86.4163

Vestad T, Marr DWM, Munakata T (2004) Flow resistance for microfluidic logic operations. Applied Physics Letters 84:5074–5075. doi: doi:10.1063/1.1764592

Xu Q, Hashimoto M, Dang TT, et al. (2009) Preparation of Monodisperse Biodegradable Polymer Microparticles Using a Microfluidic Flow-focusing Device for Controlled Drug Delivery. Small 5:1575–1581. doi: 10.1002/smll.200801855